ISSN 1064-2269, Journal of Communications Technology and Electronics, 2017, Vol. 62, No. 7, pp. 800–808. © Pleiades Publishing, Inc., 2017.
Original Russian Text © N.P. Kravchenko, S.V. Mukhin, S.A. Presnyakov, 2017, published in Radiotekhnika i Elektronika, 2017, Vol. 62, No. 7, pp. 693–702.

MICROWAVE ELECTRONICS

Analysis of the Dispersion Characteristics of Slow-Wave Structures with Two Microwave Propagation Channels[1]

N. P. Kravchenko[a], *, S. V. Mukhin[b], and S. A. Presnyakov[a]

[a] *Moscow Institute of Electronics and Mathematics, Higher School of Economics (National Research University), Moscow, 123458 Russia*

[b] *Moscow University of Finance and Law, Moscow, 117342 Russia*

**e-mail: natkrav@inbox.ru*

Received July 13, 2016

Abstract—Models of rectangular and axially symmetric resonator slow-wave structures, which are built using transmission matrix for determining the characteristics of the slow-wave structures in different operation modes, are investigated. Elements of the transmission matrix are determined from the results of 3D simulation with the use of the HFSS software. In the analysis of the dispersion characteristics, slow-wave structures with two microwave propagation channels are studied and simulated using a 4×4 transmission matrix.

DOI: 10.1134/S1064226917070075

INTRODUCTION

Broadening of the application range of microwave electromagnetic fields gave rise to a new set of microwave generators, converters, filters, transmission lines, and amplifiers; computer techniques for their design and calculation have evolved. In addition, the advent of new microwave devices extends the applicability limits of microwave technologies and allows their use in various fields of science and engineering.

The required heat sink in high- and intermediate-power microwave amplifiers is usually ensured by all-metal resonator slow-wave structures (SWSs). These structures are three-dimensional and, since the design of SWS-based devices with the help of rigorous electrodynamic programs requires much computational resources, it is important to develop simple and precision models of resonator SWSs.

1. MULTIPOLE REPRESENTATION OF A CELL OF THe RESONATOR SLOW-WAVE STRUCTURE

An all-metal resonator SWS is a transmission line in the form of a chain of identical cells. The cells are connected by waveguide channels conventionally divided into input and output. Since the investigated SWSs are periodic, the distance between the input and output cross sections of a cell is equal to SWS period L and the number of input channels is always equal to the number of output channels.

Total tangential fields $E_\alpha^\tau(x,y,z)$ and $H_\alpha^\tau(x,y,z)$ in the input and output cross sections are nothing but superpositions of an infinite number of modes corresponding to the waveguide channel under study.

According to [1], we have

$$\begin{aligned} &E_\alpha^\tau(x,y,z) \\ &= \sum_{n=1}^{\infty} E_{n(\alpha)}^\tau(x,y,z) = \sum_{n=1}^{\infty} a_{n(\alpha)}(z)\, e_{n(\alpha)}(x,y), \\ &H_\alpha^\tau(x,y,z) \\ &= \sum_{n=1}^{\infty} H_{n(\alpha)}^\tau(x,y,z) = \sum_{n=1}^{\infty} b_{n(\alpha)}(z)\, h_{n(\alpha)}(x,y), \end{aligned} \tag{1}$$

where $e_{n(\alpha)}(x, y)$ and $h_{n(\alpha)}(x, y)$ are the known vector functions of the electric and magnetic field distributions for the nth mode in the channel cross section, which depend on transverse coordinates x and y; $n(\alpha)$ is the number of the eigenmode in the channel with number α; and $a_{n(\alpha)}(z)$ and $b_{n(\alpha)}$ are the complex amplitudes of the functions of transverse vectors, which depend on longitudinal coordinate z.

In real calculations with the use of expansions (1), only a finite number of terms is used. Then, in each

[1] The results of this study were reported at the 2nd All-Russia Conference on Problems of Microwave Electronics, Moscow Institute of Electronics and Mathematics, Higher School of Economics (National Research University), Moscow, October 26–28, 2015.

channel with cross section S_α, N eigenmodes are summed ($n = 1, 2, \ldots N$):

$$E_\alpha^{\tau N}(x,y,z) = \sum_{n=1}^{N} a_{n(\alpha)}(z)\, e_{n(\alpha)}(x,y),$$
$$H_\alpha^{\alpha N}(x,y,z) = \sum_{n=1}^{N} b_{n(\alpha)}(z)\, h_{n(\alpha)}(x,y). \quad (2)$$

Since the SWS cell is a passive linear object, complex amplitudes $a_{n(\alpha)}(z)$ and $b_{n(\alpha)}$ at its input and output are related by a linear operator determined by transmission matrix $\mathbf{A^N}$ [2].

The relation between the field components at both boundaries $S_\alpha^{1,2}$is specified in the form

$$\begin{vmatrix} \vec{a}_1 \\ \hline \vec{b}_1 \end{vmatrix} = \mathbf{A}^N \begin{vmatrix} \vec{a}_2 \\ \hline \vec{b}_2 \end{vmatrix}, \quad (3)$$

where $\vec{a}_{1(2)}$ and $\vec{b}_{1(2)}$ are vectors compred of the complex amplitudes in cross sections $S_\alpha^{1,2}$ and

$$\mathbf{A}^N = \begin{vmatrix} \mathbf{A_{11}} & \mathbf{A_{12}} & \ldots & \mathbf{A_{12N}} \\ \mathbf{A_{21}} & \mathbf{A_{22}} & \ldots & \mathbf{A_{22N}} \\ \cdot & \cdot & \ldots & \cdot \\ \mathbf{A_{2N1}} & \mathbf{A_{2N2}} & \ldots & \mathbf{A_{2N2N}} \end{vmatrix}$$

is the linear matrix operator, which allows determining different operation modes of the SWS under study. If the elements of matrix operator $\mathbf{A}^N$ are known, the SWS becomes completelt formalized and all its thermodynamic characteristics can be determined.

The tangential field components in cross sections $S_\alpha^{1(2)}$ specified by Eq. (2) completely determine the field of the normal mode over the entire cell volume. In cross sections S_α^1 and S_α^2, they are related by the Floquet conditions [3]

$$E_\alpha^{\alpha N}(x,y,z) = E_\alpha^{\alpha N}(x,y,z+L)\exp(ih_nL),$$
$$H_\alpha^{\alpha N}(x,y,z) = H_\alpha^{\alpha N}(x,y,z+L)\exp(ihL), \quad (4)$$

where h_n is the propagation constant of the nth normal mode in a cell with period L. Condition (4) for the vectors of complex amplitudes is written with regard to (2) as

$$\begin{vmatrix} \vec{a}_2 \\ \hline \vec{b}_2 \end{vmatrix} = \begin{vmatrix} a_1 \\ \hline \vec{b}_1 \end{vmatrix} \exp(-ih_nL). \quad (5)$$

We transform Eq. (5) by excluding $\vec{a}_2$ and $\vec{b}_2$ with regard to (3) and arrive at

$$\mathbf{A}^N \begin{vmatrix} a_1 \\ \hline \vec{b}_1 \end{vmatrix} = \begin{vmatrix} a_1 \\ \hline \vec{b}_1 \end{vmatrix} \exp(-ih_nL). \quad (6)$$

Equation (6) is the algebraic formulation of the problem of eigenmodes of the investigated SWS in modeling its cell by a $2N$-pole described by linear matrix operator $\mathbf{A}^N$.

As is known, a nontrivial solution of system of equations (6) exists under the condition [4]

$$\det(\mathbf{A}^N - \lambda^N \mathbf{E}) = 0, \quad (7)$$

where $\lambda^N = \exp(-ih_nL)$ are the eigenvalues of transmission matrix $\mathbf{A}^N$, which allow us to determine propagation constants h_n of the $2N$-pole simulating the SWS cell, and $\mathbf{E}$ is the identity matrix.

According to [5], the obtained expression is, in fact, the dispersion equation for the normal modes of the $2N$-pole. The electrodynamic expression of the dispersion equation $\varphi = f(\omega)$ can be obtained from (7), since elements of matrix operator $\mathbf{A}^N$ depend on frequency ω.

The eigenvectors of transmission matrix $\mathbf{A}^N$ together with Eq. (2) determine the transverse electromagnetic fields corresponding to the eigenmodes in the $2N$-pole simulating the SWS cell and can be used to determine the characteristic impedance of the transmission line.

Thus, the electrodynamic characteristics of the SWS can be determined from the known elements of transmission matrix $\mathbf{A}^N$ obtained by means of formalization of the cell.

In turn, elements of the transmission matrix can be found by solving a number of electrodynamic problems under certain boundary conditions specified in the input and output waveguide channels. Methods for solution of these problems are considered in the next section.

2. METHOD FOR DETERMINING THE ELEMENTS OF THE MATRIX OPERATOR OF THE $2N$-POLE DESCRIBING THE CHARACTERISTICS OF THE SLOW-WAVE STRUCTURES

The finite-element method (FEM) is one of the most powerful and universal instruments for numerical solution of the equations of mathematical physics, which can be used to solve the electrodynamic problems in time and frequency domains [6].

The method is based on partitioning the calculated regions into many subregions (the so-called finite elements (FEs)). The field in each element is represented by means of expansion in terms of a certain system of linearly independent finite functions. These functions are nonzero only within the element volume. The shape of FEs can vary; however, for any element shape, the calculated region should be densely covered by a set of FEs without overlaps and gaps. This condition is satisfied, e.g., by tetrahedra, hexahedra, octahedra, and prisms. In the regions of the expected fast-

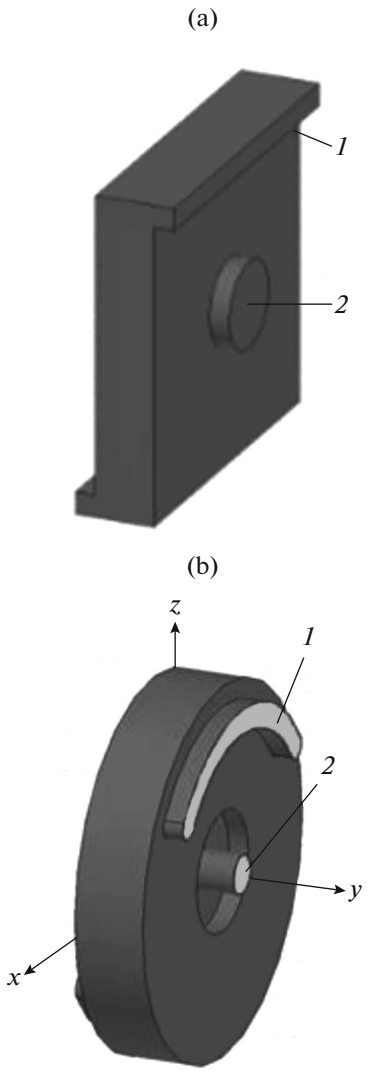

Fig. 1. (a) Rectangular and (b) axially symmetric slow-wave structures: (*1*) first and (*2*) second ports.

est variation of the electromagnetic field, the finite-element grid can have irregularities and clusterings.

As a rule, the electromagnetic field in FEs is approximated by polynomials of different orders; in this case, the expansion coefficients are equal to the values of the investigated field at the FE vertices or on FE edges. A system of equations for these coefficients can be formed using the variational technique; solving this system, one can obtain the desired potential strengths at the vertices or on the edges, which allows approximate recovering of the field over the entire investigated area.

Relative complexity of the algorithm and large memory volume required for solving the problem by the FEM are compensated by the possibility of sufficiently exact approximation of the boundaries and simulation of the fields in the regions filled with inhomogeneous and anisotropic media, as well as by the relatively small time required for solving the problem. This method has many modifications; therefore, to solve a specific class of problems, its optimum implementation can be chosen.

This method was used in the HFSS (High Frequency Structures Simulation) software, which contains two basic techniques for calculating three-dimensional models (Eigenmode Solution and Driven Modal Solution).

Simulation with the HFSS software includes specification of the so-called primitives and subsequent operations with them. The primitives can be two- and three-dimensional. The two-dimensional primitives are line, rectangle, circle, arbitrary polygon, and ellipse. The three-dimensional primitives are cube, parallelepiped, cylinder, cylinder with an arbitrary number of directrices, cone, sphere, and torus. A primitive is simulated in the three-dimensional space using cursor control keys; then, its lengths along three coordinate axes and coordinates of its reference point can be changed. This allows any variations in the sizes of a primitive and its displacement. In addition, a primitive can be copied, rotated by a certain angle, and specularly reflected. In addition, there is a special tool for rounding the primitive angles. The primitives can be combined, subtracted, or crossed. Using these operations, one can form a complex three-dimensional model, e.g., the model of a periodic SWS, from simple primitives. This model is built from several cylinders and parallelepipeds, which should be correctly subtracted from each other. Then, individual elements are combined into one cell, which is copied 12 times; after that, each second cell should be rotated by 180° to obtain the correct position of connecting resonator sections. When the three-dimensional model is built, it is necessary to choose the material for its implementation. It should be noted that not the entire SWS is simulated, but only its part where the electromagnetic field propagates. In our case, the field propagates in vacuum; therefore, we specify vacuum as the material for our model. The next stage is specification of the boundary conditions. On default, the model boundary is a perfect metal wall that does not transmit the electromagnetic field. This condition completely meets the requirements of the problem under investigation. Note that sometimes magnetic walls transparent for the field can be specified. This is used, e.g., to decrease the calculation time when the specified model is symmetric.

The calculation using the Driven Modal technique suggests simulation of one cell of the system under study (Figs. 1a and 1b); in this case, the input and output system ports should be specified (this method is universal and can be used not only in calculation of the SWS). The port is a point where the specified three-dimensional model is connected to an infinite waveguide through which the input signal is supplied and the output signal is extracted. Along with the ports, it is necessary to specify the frequency range in which the system will be calculated and the step of variation in the calculation frequency within this range. When all these conditions are specified, the system is calcu-

lated as in the Eigenmode technique, but, in contrast to the latter, after partitioning in tetrahedra, the calculation is made separately for each frequency from this range. As a result, we obtain the scattering matrix (S matrix) and the Z and Y matrices equivalent to it, which will be used to calculate the dispersion characteristics of the SWS. Figures 1a and 1b show cells of rectangular and axially symmetric SWSs obtained by cutting along the coupling slots.

3. PROGRAM FOR PROCESSING OF THE DATA OF THREE-DIMENSIONAL SIMULATION

In this study, we investigate resonator SWSs with two microwave propagation channels, i.e., the SWSs simulated in the HFSS software by four-port cells. The initial data are a set of Z-matrices obtained for the frequency set specified in the HFSS.

Along with standard data input and output stages, the processing algorithm contains the following stages:

(i) Transformation of the Z matrix to the A matrix.

(ii) Determination of the eigenvalues and eigenvectors of the A matrix.

(iii) Calculation of the dispersion and characteristic impedance of the SWS.

The results of three-dimensional simulation are processed using the MathCAD software. Let us consider the program that describes the SWS represented in the form of a four-port network [7].

The system period and the number of frequencies used in calculation are specified. The period is determined by longitudinal dimension L of the simulated cell. The number of frequencies is determined by the step of variation of the calculation frequency in the HFSS software. In the MathCAD software, this value is specified as number of steps N.

A set of frequencies and a set of Z matrices corresponding to these frequencies are chosen from the table read from the file; in this case, $z11_j$, $z12_j$, $z13_j$, $z14_j$, $z21_j$, $z22_j$, $z23_j$, $z24_j$, $z31_j$, $z32_j$, $z33_j$, $z34_j$, $z41_j$, $z42_j$, $z43_j$, and $z44_j$ are the elements of the jth Z matrix and ω_j is the calculated frequency. To transform the Z matrices into equivalent A matrices, we used the transition matrix (see Appendix). When the desired A matrix is obtained, we can calculate its eigenvalues using the function

$$\mathbf{LV}_j = \text{eigenvals}(\mathbf{A0}_j). \tag{8}$$

The eigenvalues are complex numbers. In this case, the A matrix dimensionality is 4 × 4; therefore, we obtain four eigenvalues, which are pairwise complex conjugate.

The first pair of solutions corresponds to the forward and backward waves propagating along the SWS slot channel; the second pair corresponds to the waves propagating along the transit channel. Each eigenvalue of the A matrix has its own eigenvector, which allows determining voltages and currents in the port cross sections; the latter parameters, in turn, allow finding the characteristic impedance of the mode.

The eigenvectors are determined as

$$\begin{aligned} \mathbf{VV}_j &= \text{eigenvec}[\mathbf{A0}_j,(\mathbf{LV}_j)_0] \quad \mathbf{VV1}_j = \text{eigenvec}[\mathbf{A0}_j,(\mathbf{LV}_j)_1], \\ \mathbf{VV2}_j &= \text{eigenvec}[\mathbf{A0}_j,(\mathbf{LV}_j)_2] \quad \mathbf{VV3}_j = \text{eigenvec}[\mathbf{A0}_j,(\mathbf{LV}_j)_3]. \end{aligned} \tag{9}$$

These eigenvectors can be used to determine characteristic impedances of the ports:

$$\mathbf{ZR}_j = \text{Re}\left[\frac{1}{\frac{(\mathbf{VV}_j)_0}{(\mathbf{VV}_j)_1}+\frac{(\mathbf{VV3}_j)_0}{(\mathbf{VV3}_j)_1}+\frac{(\mathbf{VV1}_j)_0}{(\mathbf{VV1}_j)_1}}\right], \tag{10}$$

$$\mathbf{ZIR}_j = \text{Im}\left[\frac{1}{\frac{(\mathbf{VV}_j)_0}{(\mathbf{VV}_j)_1}+\frac{(\mathbf{VV3}_j)_0}{(\mathbf{VV3}_j)_1}+\frac{(\mathbf{VV1}_j)_0}{(\mathbf{VV1}_j)_1}}\right], \tag{11}$$

$$\mathbf{ZR1}_j = \text{Re}\left[\frac{1}{\frac{(\mathbf{VV}_j)_0}{(\mathbf{VV}_j)_1}+\frac{(\mathbf{VV3}_j)_0}{(\mathbf{VV3}_j)_1}+\frac{(\mathbf{VV2}_j)_0}{(\mathbf{VV2}_j)_1}}\right], \tag{12}$$

$$\mathbf{ZIR1}_j = \text{Im}\left[\frac{1}{\frac{(\mathbf{VV}_j)_0}{(\mathbf{VV}_j)_1}+\frac{(\mathbf{VV3}_j)_0}{(\mathbf{VV3}_j)_1}+\frac{(\mathbf{VV2}_j)_0}{(\mathbf{VV2}_j)_1}}\right], \tag{13}$$

$$\mathbf{ZR2}_j = \text{Re}\left[\frac{1}{\frac{(\mathbf{VV}_j)_3}{(\mathbf{VV}_j)_2}+\frac{(\mathbf{VV3}_j)_3}{(\mathbf{VV3}_j)_2}+\frac{(\mathbf{VV1}_j)_3}{(\mathbf{VV1}_j)_2}}\right], \tag{14}$$

$$\mathbf{ZIR2}_j = \text{Im}\left[\frac{1}{\frac{(\mathbf{VV}_j)_3}{(\mathbf{VV}_j)_2}+\frac{(\mathbf{VV3}_j)_3}{(\mathbf{VV3}_j)_2}+\frac{(\mathbf{VV1}_j)_3}{(\mathbf{VV1}_j)_2}}\right], \tag{15}$$

$$\mathbf{ZR3}_j = \mathrm{Re}\left[\frac{1}{\frac{(\mathbf{VV}_j)_3}{(\mathbf{VV}_j)_2} + \frac{(\mathbf{VV3}_j)_3}{(\mathbf{VV3}_j)_2} + \frac{(\mathbf{VV2}_j)_3}{(\mathbf{VV2}_j)_2}}\right], \quad (16)$$

$$\mathbf{ZIR3}_j = \mathrm{Im}\left[\frac{1}{\frac{(\mathbf{VV}_j)_3}{(\mathbf{VV}_j)_2} + \frac{(\mathbf{VV3}_j)_3}{(\mathbf{VV3}_j)_2} + \frac{(\mathbf{VV2}_j)_3}{(\mathbf{VV2}_j)_2}}\right]. \quad (17)$$

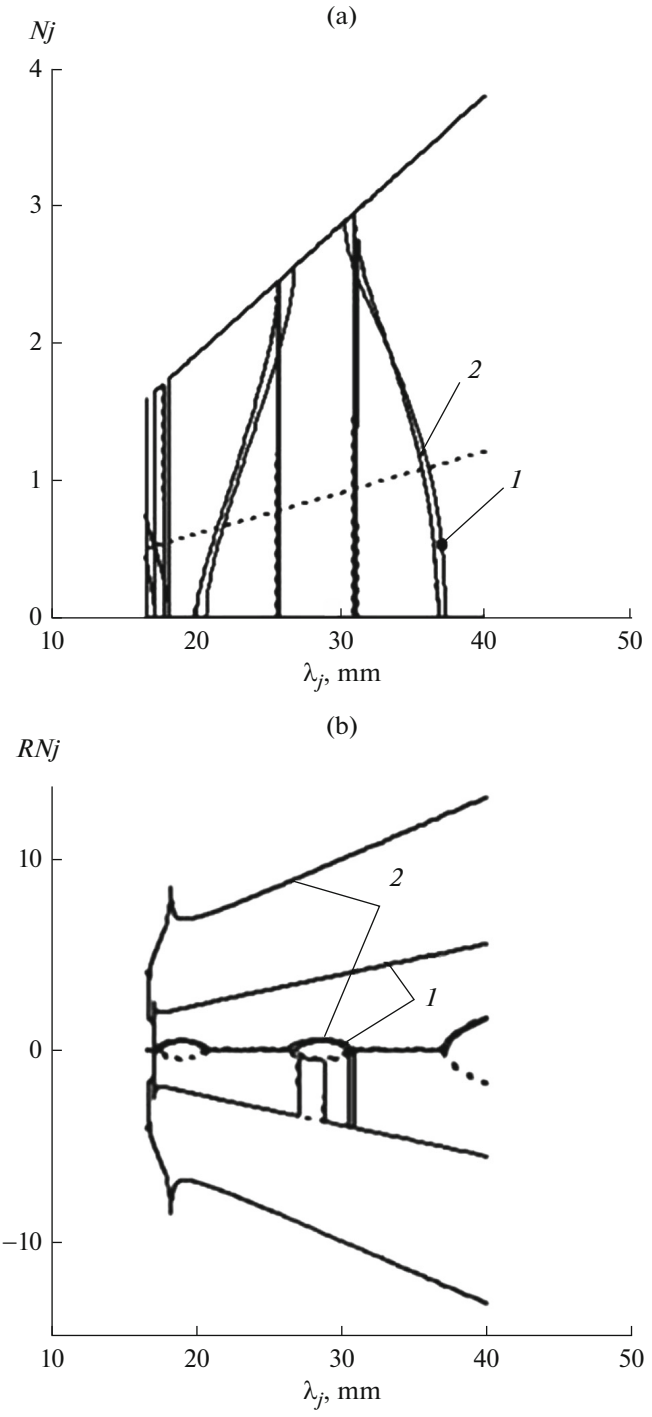

Fig. 2. (a) Slowing factor *Nj* and (b) reactive attenuation *RNj* of a cell of the rectangular resonator SWS formed by cutting along the coupling slots for transit channel radii r_1 = (*1*) 0.75 and (*2*) 2 mm.

4. ANALYSIS OF DISPERSION CHARACTERISTICS OF THE RESONATOR SLOW-WAVE STRUCTURES

In this study, we investigate the SWSs shown in Figs. 1a and 1b. These structures are resonator SWSs with two microwave propagation channels. The SWS cells, which can be simulated using the Driven Modal technique, are formed by cutting the rectangular or axially symmetric SWSs along the coupling slots.

Calculation of the SWS dispersion characteristics of the yields four solutions (modes). The first pair of solutions corresponds to the forward and backward waves propagating along the SWS slot channel (Figs. 2a and 3a) and the second pair corresponds to the transit-channel waves (Figs. 2b and 3b). The phase shift per the cell in the transit channel is either 0 or π and can change stepwise by $\pm\pi$. The wavenumbers of these waves are complex; the real part determines the reactive attenuation in the stopbands and the transit channel (see Fig. 2b). As the transit channel radius increases, the π-shape of the fundamental dispersion characteristic shifts toward the low-frequency region (Figs. 2a and 2b).

Analogous dispersion characteristics were calculated for the axially symmetric resonator SWSs (Figs. 3a and 3b). As in the rectangular SWSs, the dispersion characteristics of the axially symmetric SWSs have four solutions (modes). The wave numbers of these solutions are complex; the real part determines the reactive attenuation in the stopbands and the transit channel. The phase shift per one cell in the transit channel of the axially symmetric SWSs is analogous to the case of the rectangular SWSs. As the transit channel radius increases, the fundamental dispersion characteristic shifts toward the low-frequency region (Figs. 3a and 3b).

Characteristic impedances of the SWS ports are determined from formulas (10)–(17) and are complex. The characteristic impedance of the slot channel of the resonator SWS is presented in Figs. 4a and 4b. Characteristic impedances of the slot and transit channels of the axially symmetric SWS are shown in Figs. 5a and 5b.

As the transit channel radius increases, the characteristic impedance of the slot channel is transformed. It becomes complex in the passbands and singularities at their boundaries disappear. Beyond the passbands, the characteristic impedance remains purely imagi-

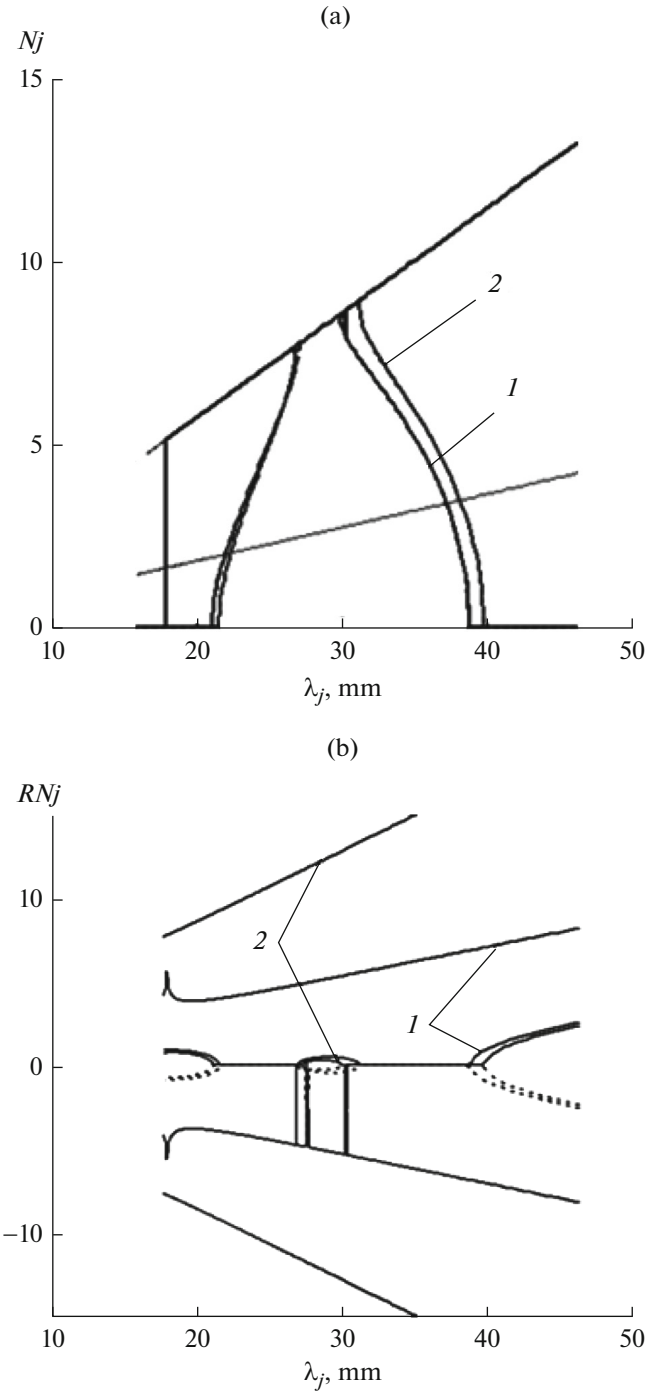

Fig. 3. (a) Slowing factor *Nj* and (b) reactive attenuation *RNj* of a cell of the axially symmetric resonator SWS formed by cutting along the coupling slots for transit channel radii r_1 = (*1*) 0.75 and (*2*) 2 mm.

nary and has a limited value. The characteristic impedance of the transit channel remains complex.

CONCLUSIONS

The results obtained have shown that the account for the transit channel significantly changes the dispersion characteristics of the resonator SWSs, even for small transit channel radii. The complex value of the characteristic impedance and the absence of singularities at the passband boundaries make it possible to uniformly describe amplification in the passband and at its boundaries.

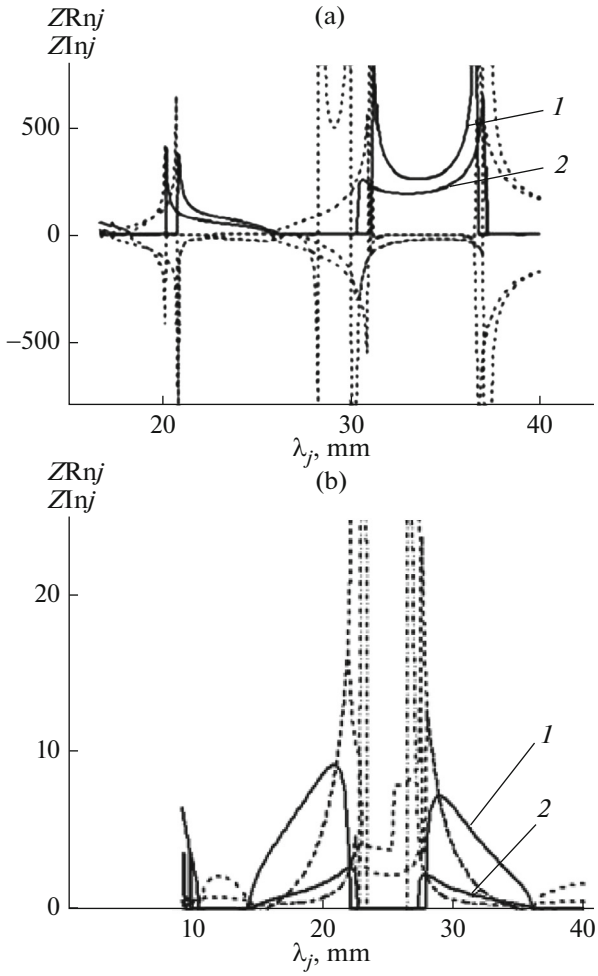

Fig. 4. (solid curves) Real $Z\mathrm{R}nj$ and (dashed curves) imaginary $Z\mathrm{I}nj$ parts of the characteristic impedance of (a) the slot ($n = 0.1$) and (b) the transit ($n = 2, 3$) channels of the rectangular SWS partitioned into cells along the coupling slots for transit channel radii $r_1 =$ (*1*) 0.75 and (*2*) 2 mm.

APPENDIX

Matrix of transition from impedance matrix Z to transmission matrix A:

$$\mathbf{A0}_j := \begin{pmatrix} \dfrac{z22_j}{z12_j} - \dfrac{z32_j \cdot z24_j - \dfrac{z32_j \cdot z22_j \cdot z14_j}{z12_j}}{z34_j \cdot z12_j - z14_j \cdot z32_j} & z21_j + \dfrac{z11_j \cdot z22_j}{z12_j} + \dfrac{-z24_j \cdot z11_j \cdot z32_j + z24_j \cdot z31_j \cdot z12_j}{z34_j \cdot z12_j - z14_j \cdot z32_j} + \dfrac{z22_j \cdot z11_j \cdot z32_j \cdot \dfrac{z14_j}{z12_j} - z31_j \cdot z22_j \cdot z14_j}{z34_j \cdot z12_j - z14_j \cdot z32_j} \\ \dfrac{1}{z12_j} + \dfrac{z32_j \cdot z14_j}{z34_j \cdot z12_j \cdot z12_j - z14_j \cdot z32_j \cdot z12_j} & \dfrac{z11_j}{z12_j} + \dfrac{z11_j \cdot z14_j \cdot z32_j - z31_j \cdot z12_j \cdot z14_j}{z34_j \cdot z12_j \cdot z12_j - z14_j \cdot z32_j \cdot z12_j} \\ \dfrac{z42_j}{z12_j} + \dfrac{\dfrac{z14_j \cdot z42_j \cdot z32_j}{z12_j} - z32_j \cdot z44_j}{z34_j \cdot z12_j - z14_j \cdot z32_j} & \dfrac{z42_j \cdot z11_j \cdot z34_j - z42_j \cdot z14_j \cdot z31_j - z32_j - z32_j \cdot z44_j \cdot z11_j + \dfrac{z32_j \cdot z44_j \cdot z14_j \cdot z31_j}{z34_j}}{z12_j \cdot z34_j - z14_j \cdot z32_j} - z41_j + \dfrac{z31_j \cdot z44_j}{z34_j} \\ \dfrac{-z32_j}{z34_j \cdot z12_j - z14_j \cdot z32_j} & \dfrac{\dfrac{-z11_j \cdot z32_j}{z34_j \cdot z12_j} + \dfrac{z31_j}{z34_j}}{1 - \dfrac{z14_j \cdot z32_j}{z34_j \cdot z12_j}} \end{pmatrix}$$

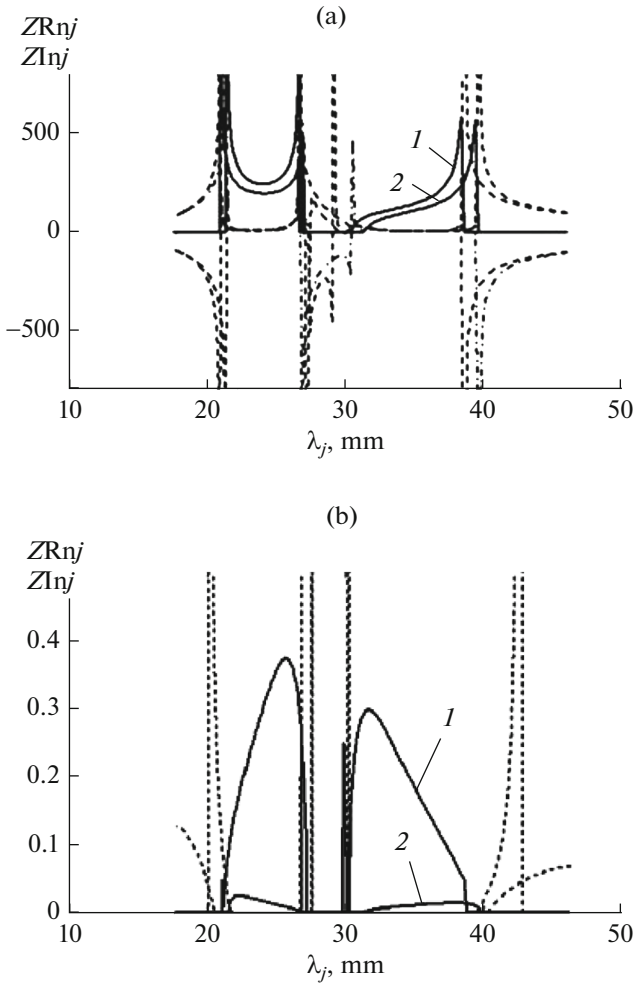

Fig. 5. (solid curves) Real $Z\mathrm{R}nj$ and (dashed curves) imaginary $Z\mathrm{I}nj$ parts of the characteristic impedance of (a) the slot ($n = 0, 1$) and (b) the transit ($n = 2, 3$) channels of the axially symmetric resonator partitioned into cells along the coupling slots for transit channel radii $r_1 =$ (*1*) 0.75 and (*2*) 2 mm.

$$\begin{pmatrix} \dfrac{z12_j \cdot z24_j - z22_j \cdot z14_j}{z34_j \cdot z12_j - z14_j \cdot z32_j} & -z23_j + \dfrac{z22_j \cdot z13_j}{z12_j} + \dfrac{-z13_j \cdot z32_j \cdot z24_j + z33_j \cdot z12_j \cdot z24_j + \dfrac{z32_j \cdot z13_j \cdot z22_j \cdot z14_j}{z12_j} - z33_j \cdot z22_j \cdot z14_j}{z34_j \cdot z12_j - z14_j \cdot z32_j} \\ \dfrac{-z14_j}{z34_j \cdot z12_j - z14_j \cdot z32_j} & \dfrac{z13_j}{z12_j} + \dfrac{-z33_j \cdot z12_j \cdot z14_j + z13_j \cdot z32_j \cdot z14_j}{z34_j \cdot z12_j \cdot z12_j - z14_j \cdot z32_j \cdot z12_j} \\ \dfrac{z12_j \cdot z44_j - z14_j \cdot z42_j}{z34_j \cdot z12_j - z14_j \cdot z32_j} & \dfrac{-z13_j \cdot z32_j \cdot z44_j + z34_j \cdot z13_j \cdot z42_j + \dfrac{z33_j \cdot z32_j \cdot z14_j \cdot z44_j}{z34_j} - z33_j \cdot z14_j \cdot z42_j}{z34_j \cdot z12_j - z14_j \cdot z32_j} - z43_j + \dfrac{z33_j \cdot z44_j}{z34_j} \\ \dfrac{1}{z34_j - \dfrac{z14_j \cdot z32_j}{z12_j}} & \dfrac{\dfrac{-z13_j \cdot z32_j}{z34_j \cdot z12_j} + \dfrac{z33_j}{z34_j}}{1 - \dfrac{z14_j \cdot z32_j}{z34_j \cdot z12_j}} \end{pmatrix}$$

ACKNOWLEDGMENTS

This study was supported by the Program "Scientific Fund Program of the Higher School of Economics (National Research University)" for years 2017–2018 (grant no. 17-05-0009) and by the State Program for Support of the Largest Russian Institutes of Higher Education (Project 5–10).

REFERENCES

1. V. V. Nikol'skii, *Decomposition Approach to Electrodynamics Problems* (Nauka, Moscow, 1983), p. 30 [in Russian].
2. V. V. Nikol'skii, Izv. Vyssh. Uchebn. Zaved. Radiofiz. **20**, 5 (1977).
3. P. E. Krasnushkin, Zh. Tekh. Fiz., **17**, 705 (1947).
4. D. A. Watkins, *Topics in Electromagnetic Theory* (Wiley, New York, 1958).
5. R. A. Silin and V. P. Sazonov, *Slow-Wave Structures* (Sovetskoe Radio, Moscow, 1966), p. 632 [in Russian].
6. J.-C. Sabonnadiere and J.-L. Coulomb, *La methode des elements finis Du modele. a la CAO* (Paris, Hermes, 1986; Mir, Moscow, 1989).
7. S. V. Mukhin and A. V. Panov, in *Proc. 10th Int. Sci.-Eng. Conf. on Actual Problems of Electronic Instrument Making (APEIM 2012), Saratov, Sept. 19–20, 2012* (Saratov. Gos. Techn. Univ., Saratov, 2012), p. 203.

Translated by E. Bondareva